Thermal Buckling Analysis of Moderately Thick Composite Cylindrical Shells under Axisymmetric Thermal Loading

M. Darvizeh[1], A. Darvizeh[2], A.R. Shaterzadeh[3], and R. Ansari [4]
Mech. Eng. Group, Guilan Univ.

ABSTRACT
In this paper, a semi-analytical finite element method is presented to study the thermal buckling behavior of moderate-thick cylindrical shells. The theory is formulated based on first shear deformation assumptions. Simplified Sanders theory and non simplified theory are employed for calculation of geometrical stiffness matrix. The results obtained from these two theories are compared which shows that the critical thermal buckling temperature based on non-simplified theory is higher than that of the simplified Sanders theory. The material is high strength carbon and the boundary condition is clamped-clamped. The influence of fiber angle orientations is also studied.

Key Words: Semi-analytical Finite Element Method, Thermal Load, Axisymmetric Temperature

تحلیل کمانش حرارتی پوسته های استوانه ای کامپوزیتی نسبتاً ضخیم تحت بار حرارتی متقارن محوری

منصور درویزه، ابوالفضل درویزه ، علیرضا شاطرزاده و رضا انصاری
گروه مهندسی مکانیک، دانشگاه گیلان

چکیده
در این مقاله، یک روش نیمه تحلیلی المان محدود برای مطالعه رفتار کمانش حرارتی پوسته‌های نسبتاً ضخیم ارائه شده است. تئوری به کار رفته بر اساس فرضیات تغییر شکل برشی مرتبه اول فرمول بندی شده است. برای محاسبه ماتریس سختی هندسی، تئوری‌های ساده شده و ساده نشده سندرز به کار رفته است. نتایج به‌دست آمده از این دو تئوری با هم مقایسه شده‌اند. مقایسه نتایج حاصل از این دو تئوری نشان می‌دهد که دمای بحرانی کمانش حرارتی در تئوری ساده نشده سندرز بالاتر است. ماده مورد بررسی کربن با مقاومت بالا و شرایط مرزی دو سر درگیر در فرض شده است . تأثیر زاویه الیاف نیز مورد مطالعه قرار گرفته است.

واژه‌های کلیدی: اجزای محدود نیمه تحلیلی، بار حرارتی، دمای متقارن محوری

1-Professor: Darvizeh@guilan.ac.ir
2-Professor
3-PhD Student (Corresponding Author): a-shaterzadeh@guilan.ac.ir
4-PhD Student

Introduction

Many key industries, such as Aero-space, automotive, military are under constant pressure to produce lighter and stronger structures. High strength and stiffness to weight ratio of composite materials are the main reasons for such demand. Superior environmental, mechanical thermal and electrical properties have made them so attractive in many applications. As pointed by Earl Thornton [1] in his recent review paper on thermal buckling of plates and shells, the availability of studies on thermal buckling in composite shells is scarce. Toorani and Lakis [2] have performed a generalization of geometrically linear shear deformation theory for multilayered anisotropic shell of general shape. Abir and Nardo [3] consider the problem of thermal buckling in thin circular cylindrical shells when there exits temperature gradients in the circumferential direction. Patel et al [4] have performed thermal buckling behavior of laminated cross-ply oval cylindrical shells using finite element approach. Ganesan and Kadoli [5] have analyzed piezoelectric composite cylindrical shells operating in a steady state axisymmetric temperature using a semi-analytical finite element method. Birman and Bert [6] considered studies on the buckling and post buckling response of composite shells subjected to high temperature using the equilibrium equations for shells under the simultaneous action of thermal and axial load.

Problem Formulation

A cylindrical shell being exposed axi-symmetric temperature is shown in Fig.**1**. The reference surface displacements according to the FSDT are expressed as [7]:

$$\begin{aligned} u &= u_0 + z\psi_s \\ v &= v_0 + z\psi_\theta \\ w &= w_0 \end{aligned} \qquad (1)$$

where u_0, v_0 and w_0 are displacement of reference surface along the s,θ,z respectively, ψ_s,ψ_θ also represent the rotations of tangent to the reference oriented along the s,θ direction respectively. The coordinate system for revolution shells represented in fig. **2**. In the semi-analytical method displacement field is assumed to depend on the circumferential direction hence the θ direction is expressed in a Fourier series given as:

$$\begin{Bmatrix} u_0 \\ v_0 \\ w_0 \\ \psi_s \\ \psi_\theta \end{Bmatrix} = \sum_{n=0}^{\infty} \begin{bmatrix} \cos n\theta & 0 & 0 & 0 & 0 \\ 0 & \sin n\theta & 0 & 0 & 0 \\ 0 & 0 & \cos n\theta & 0 & 0 \\ 0 & 0 & 0 & \cos n\theta & 0 \\ 0 & 0 & 0 & 0 & \sin n\theta \end{bmatrix} \begin{Bmatrix} u_{0n} \\ v_{0n} \\ w_{0n} \\ \psi_{sn} \\ \psi_{\theta n} \end{Bmatrix} \qquad (2)$$

Where, n indicates the circumferential mode number.

For the global revolution shells, the normal and shear strain components are related to the components of the displacement vector by:

$$\varepsilon_i = \frac{\partial}{\partial \alpha_i}\left(\frac{U_i}{\sqrt{g_i}}\right) + \frac{1}{2g_i}\sum_{k=1}^{3}\frac{\partial g_i}{\partial \alpha_k}\frac{U_k}{\sqrt{g_k}} \quad i = 1,2,3,$$

$$\gamma_{ij} = \frac{1}{\sqrt{g_i g_j}}\left[g_i \frac{\partial}{\partial \alpha_j}\left(\frac{U_i}{\sqrt{g_i}}\right) + g_j \frac{\partial}{\partial \alpha_i}\left(\frac{U_j}{\sqrt{g_j}}\right)\right], \quad i,j = 1,2,3 \; ; i \neq j \qquad (3)$$

Where,

$$\alpha_1 = s, \alpha_2 = \theta, \alpha_3 = z, u_1 = u, u_2 = v, u_3 = w$$

and,

$$g_1 = A_1^2\left(1 + \frac{z}{R_1}\right)^2, g_2 = A_2^2\left(1 + \frac{z}{R_2}\right)^2, g_3 = 1$$

where, A_i, R_i, z are the Lames parameters, the principal curvature radius and the thickness coordinate respectively and U_k

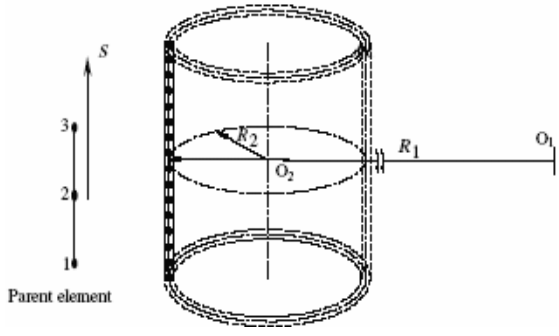

Figure (1): Schematics of the description of the cylindrical shell using three nodded quadratic line element.

is displacement component [7]. Substituting equation (1) into equation (3) the following strain displacement relations for shell space is given as:

$$\varepsilon_{ss}=\frac{1}{\left(1+\frac{z}{R_1}\right)}\left(\varepsilon_{ss}^0+z\kappa_s\right)\ ,\ \varepsilon_{\theta\theta}=\frac{1}{\left(1+\frac{z}{R_2}\right)}\left(\varepsilon_{\theta\theta}^0+z\kappa_\theta\right)$$

$$\gamma_{s\theta}=\frac{1}{\left(1+\frac{z}{R_1}\right)}\left(\gamma_s^0+z\tau_s\right)+\frac{1}{\left(1+\frac{z}{R_2}\right)}\left(\gamma_\theta^0+z\tau_\theta\right)$$

$$\gamma_{sz}=\frac{1}{\left(1+\frac{z}{R_1}\right)}\mu_s^0\ \ ,\ \ \gamma_{\theta z}=\frac{1}{\left(1+\frac{z}{R_2}\right)}\mu_\theta^0 \tag{4}$$

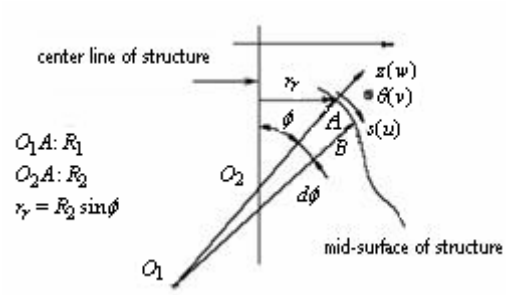

Figure (2): Coordinate system for revolution shells.

where, $\varepsilon_{ss},\gamma_{s\theta},\gamma_{sz}$ are the normal and shearing strains and $\varepsilon_{ss}^0,\varepsilon_{\theta\theta}^0,\gamma_s^0,\gamma_\theta^0$ are the in-plane normal and in-plane shearing strains respectively. $\kappa_s,\kappa_\theta,\tau_s,\tau_\theta,\mu_s^0,\mu_\theta^0$ also are the change in the curvature and torsion of the reference surface and the shearing strain components respectively. In the special case for cylindrical shell we have:

$$A_1=1\ \ ,\ \ A_2=R\ \ ,\ \ \frac{1}{R_1}=0\ \ ,\ \ R_2=R \tag{5}$$

Stiffness matrix

Potential energy continuum elastic structure is defined as the sum of the strain energy and the potential work, as:

$$\Pi\ =\ U\ +\ W\ . \tag{6}$$

For semi-analytical investigation an isoparametric element with three nodes is used in the axial direction. Fig.**1** represents the cylindrical shell using this type of element, where each node has five degree of freedom.

The displacement parameters associated with the element are as:

$$\{d_e\}^T=\left\{\begin{matrix}u_1,v_1,w_1,\psi_{s1},\psi_{\theta1},u_2,v_2,w_2\\,\psi_{s2},\psi_{\theta2},u_3,v_3,w_3,\psi_{s3},\psi_{\theta3}\end{matrix}\right\}. \tag{7}$$

The subscripts 1, 2, 3 stand for the three nodes of the element. The shape function N_i in terms of the axial coordinate are given by

$$N_1=\frac{s^2-sl}{2l^2}\ \ ,\ \ N_2=\frac{l^2-s^2}{l^2}\ \ ,\ \ N_3=\frac{s^2+sl}{2l^2}, \tag{8}$$

where, l indicates the length of element. From the strain energy relation given as:

$$U=\frac{1}{2}\int_A\sigma^T\varepsilon dA=\frac{1}{2}\{d_e\}^T[K_e]\{d_e\}\ . \tag{9}$$

The stiffness matrix $[K_e]$, of each element is obtained as:

$$[K_e]=\int_0^{2\pi}\int_0^l[B]^T[D][B]\,R\,ds\,d\theta\ . \tag{10}$$

The strain-displacement matrix $[B]$,is expressed in terms of the interpolation function and their derivatives . The constitutive matrix $[D]$ consist of various integrated shell stiffness: $A_{ij},B_{ij},D_{ij},E_{ij}\ ,F_{ij}\ ,C_{ij}$ .The matrix $[B]$ and $[D]$ are given in appendix. Various integrated shell stiffness are defined as follows:

$$(A_{ij},B_{ij},D_{ij},E_{ij},F_{ij},C_{ij})=\sum_{k=1}^{N}\int_{z_{k-1}}^{z_k}(\overline{Q_{ij}})_k(1,z,z^2,z^3,z^4,z^5)dz \tag{11}$$

where, $\overline{Q_{ij}}$ are the reduced stiffness coefficients and N is the number of lamina. More elaborate details on the above discussion are given in the article presented by Toorani and Lakis [2].

Geometric Stiffness Matrix

The strain vector $\{\varepsilon_0\}$ due to temperature is represented as:

$$\{\varepsilon_0\} = \begin{Bmatrix} \overline{\varepsilon}_{ss} \\ \overline{\varepsilon}_{\theta\theta} \\ \overline{\varepsilon}_{zz} \\ \overline{\gamma}_{s\theta} \\ \overline{\gamma}_{sz} \\ \overline{\gamma}_{\theta z} \end{Bmatrix} = \Delta T \begin{Bmatrix} \alpha_s \\ \alpha_\theta \\ 0 \\ \alpha_{s\theta} \\ 0 \\ 0 \end{Bmatrix}, \qquad (12)$$

where, ΔT is the rise in temperature and using Fourier series. The rise temperature in the circumferential direction is:

$$\Delta T = \sum_{n=0}^{\infty} \Delta T_n \cos n\theta . \qquad (13)$$

$\alpha_s, \alpha_\theta, \alpha_{s\theta}$ are thermal expansion coefficients in the shell co-ordinates and can be related to the thermal expansion coefficients (α_1, α_2) in the material principal directions, as:

$$\begin{aligned} \alpha_s &= \alpha_1 \cos^2 \upsilon + \alpha_2 \sin^2 \upsilon \\ \alpha_\theta &= \alpha_1 \sin^2 \upsilon + \alpha_2 \cos^2 \upsilon \\ \alpha_{s\theta} &= 2(\alpha_1 - \alpha_2)\cos\upsilon \sin\upsilon \end{aligned} \qquad (14)$$

where, υ is the lamina orientation angle.
The work done by the initial state of stress due to the applied thermal field is given as:

$$W = \int_V \left(\sigma^0_{ss}\varepsilon^{NL}_{ss} + \sigma^0_{\theta\theta}\varepsilon^{NL}_{\theta\theta} + \tau^0_{s\theta}\gamma^{NL}_{s\theta}\right) dV \qquad (15)$$

The non-linear strain components are defined as:

$$\begin{aligned} \varepsilon^{NL}_{ss} &= \frac{1}{2}\left(\left(\frac{\partial u}{\partial s}\right)^2 + \left(\frac{\partial v}{\partial s}\right)^2 + \left(\frac{\partial w}{\partial s}\right)^2\right) \\ \varepsilon^{NL}_{\theta\theta} &= \frac{1}{2}\left(\frac{1}{R(1+z/R)}\right)^2 \left(\left(\frac{\partial v}{\partial \theta} + w\right)^2 \right. \\ &\left. + \left(\frac{\partial v}{\partial \theta}\right)^2 + \left(\frac{\partial w}{\partial \theta} - v\right)^2\right) \\ \gamma^{NL}_{s\theta} &= \left(\frac{1}{R(1+z/R)}\right)\left(\left(\frac{\partial u}{\partial s}.\frac{\partial u}{\partial \theta}\right) + \right. \\ &\left. \left(\frac{\partial v}{\partial s}\right).\left(\frac{\partial v}{\partial \theta} + w\right) + \left(\frac{\partial w}{\partial s}\right)\left(\frac{\partial w}{\partial \theta} - v\right)\right) \end{aligned} \qquad (16)$$

In the simplified Sanders theory [4] the non-linear strain component are define as:

$$\begin{aligned} \varepsilon^{NL}_{ss} &= \frac{1}{2}\left(\frac{\partial w}{\partial s}\right)^2 \\ \varepsilon^{NL}_{\theta\theta} &= \frac{1}{2}\left(\frac{1}{R(1+z/R)}\right)^2 \left(\frac{\partial w}{\partial \theta} - v\right)^2 \\ \gamma^{NL}_{s\theta} &= \left(\frac{1}{R(1+z/R)}\right)\left(\frac{\partial w}{\partial s}\right)\left(\frac{\partial w}{\partial \theta} - v\right) \end{aligned} \qquad (17)$$

Using Eq. (6) and considering the thermal effect, the total potential energy is given as;

$$\begin{aligned} \Pi = &\frac{1}{2}\{d_e\}^T [K_e]\{d_e\} + \frac{1}{2}\{d_e\}^T [K_{Ge}]\{d_e\} \\ &- \{d_e\}^T \{F^{th}_e\} + \frac{1}{2}\int_A \{\varepsilon_0\}^T [D]\{\varepsilon_0\}\, dA \end{aligned} \qquad (18)$$

where, $[K_{Ge}]$ and $\{F^{th}_e\}$ are, respectively, element geometric stiffness matrix and element thermal load vector and defined as:

$$[K_{Ge}] = \int\int \left[\sum_{k=1}^{N}\int_{z_{k-1}}^{z_k} [B^*]^T [Z]^T [S][Z][B^*]\left(1+\frac{z}{R}\right) dz\right] R\, ds\, d\theta , \qquad (19)$$

$$\{F^{th}_e\} = \int\int \left[\sum_{k=1}^{N}\int_{z_{k-1}}^{z_k} [B]^T [\overline{Z}]^T [\overline{Q}_{ij}]\{\varepsilon_0\}\left(1+\frac{z}{R}\right) dz\right] R\, ds\, d\theta , \qquad (20)$$

where the sub matrices $[Z]$ and $[\overline{Z}]$ are defined as follows:

$$\begin{aligned} [Z] &= [Z_1 \quad zZ_1] \\ [\overline{Z}] &= \begin{bmatrix} Z_1 & zZ_1 \\ O_1 & O_1 \end{bmatrix} \end{aligned} \qquad (21)$$

$$Z_1 = \begin{bmatrix} 1 & 0 & 0 & 0 & 0 \\ 0 & \frac{1}{(1+z/R)} & 0 & 0 & 0 \\ 0 & 0 & 1 & 0 & 0 \\ 0 & 0 & 0 & \frac{1}{(1+z/R)} & 1 \end{bmatrix}, \qquad (22)$$

and O_1 is null matrix of size 2*5.

Submatrix $[S]$ consists of the normal and shear stresses. The strain-displacement matrix $[\ B^*\ ]$ is expressed in terms of the interpolation function and their derivatives according to non-linear strains.
One can also find more elaborate details on the above discussion in the article presented by B.P Patel et al. [4].

The stress resultants are given by [7]:

$$\begin{Bmatrix} N_s \\ N_{s\theta} \\ Q_s \\ M_s \\ M_{s\theta} \end{Bmatrix} = \int_z \begin{Bmatrix} \sigma_s \\ \tau_{s\theta} \\ \tau_{sz} \\ z\sigma_s \\ z\tau_{s\theta} \end{Bmatrix} \left(1 + \frac{z}{R_2}\right) dz \qquad (23)$$

$$\begin{Bmatrix} N_\theta \\ N_{\theta s} \\ Q_\theta \\ M_\theta \\ M_{\theta s} \end{Bmatrix} = \int_z \begin{Bmatrix} \sigma_\theta \\ \tau_{\theta s} \\ \tau_{\theta z} \\ z\sigma_\theta \\ z\tau_{\theta s} \end{Bmatrix} \left(1 + \frac{z}{R_1}\right) dz$$

The quantities ($N_s, N_\theta, N_{s\theta}, N_{\theta s}$) are called the in-plane stress resultant, and ($M_s, M_\theta, M_{s\theta}, M_{\theta s}$) are called the stress coupled resultants ;(Q_s, Q_θ) denote the transverse force resultants.

Using the following approximation:

$$\frac{1}{\left(1 + \frac{z}{R}\right)} \cong 1 - \frac{z}{R} + \left(\frac{z}{R}\right)^2 \mp \ldots \qquad (24)$$

We can write:

$$[K_{Ge}] = \iint [B^*]^T [N^{th}] [B^*] R ds d\theta\ , \qquad (25)$$

where, $[\ N^{th}\ ]$ represents the stress vectors.
Minimization of Π with respect to the displacement vector $\{d_e\}$ leads to the following standard equation:

$$[K_e]\{d_e\} - \{F_e^{th}\} = 0\ . \qquad (26)$$

Using Eq. (26) the displacement vector is computed and then vector of stresses and moment resultants are evaluated as follows:

$$\{N_s\ N_{s\theta}\ Q_s\ N_\theta\ N_{\theta s}\ Q_\theta\ M_s\ M_{s\theta}\ M_\theta\ M_{\theta s}\}^T = [D][B]\{d_e\} - [\bar{D}]\{\varepsilon_0\} \qquad (27)$$

Where $[\bar{D}]$ is constitutive matrix according to thermal load vector.
The stress resultants are found for each element and are used in Eq. (25) to compute the geometric stiffness matrix.

Discussion

The present formulation is developed for thermal buckling analysis of composite shells with non-simplified and simplified Sanders theories. In this study High strength carbon-Graphite/Epoxy composite cylindrical shell with $l/R = 1.048$ and clamped-clamped boundary conditions is utilized .The critical buckling temperatures are obtained based on the variation of circumferential mode numbers from 1 to 25. This is defined as the difference between ambient ($20^\circ C$) and the final temperature. Temperature distribution in cylindrical shell is assumed to be axi-symmetric.
The geometric details of the composite shell considered for the study are given in table 1.The properties of High strength carbon-Graphite/Epoxy material are listed in table 2.
Static thermal buckling analysis is carried out using the following equation:

$$([\ K^{UU}\ ] - \Delta T[\ K_G^{*UU}\ ])\{\delta\} = 0\ . \qquad (28)$$

Table (1): Details of cylindrical shell.

Length (m)	Radius (m)	Thickness (m)	B.C
0 .914	0.876	0.0030	C-C

In the Eq. (28) $[\ K^{UU}\ ]$ is the global Structural stiffness matrix and $[\ K_G^{*UU}\ ]$ is the global geometric stiffness matrix due to unit temperature rise. ΔT is the buckling eigenvalues and $\{\delta\}$ is the corresponding buckling eigenvector.
The critical buckling temperature of composite cylindrical shell with $l/R = 1.048$ and for different fiber angle and two theories are plotted with respect to circumferential harmonic, refer to Figs.**2-6**. The lowest critical buckling modes for two theories are listed in table 3.

Table (2): Material properties High strength carbon-Graphite/Epoxy.

Young Modulus (GPa)	E_{11}, E_{22}, E_{33}	181, 10.34, 10.34
Shear Modulus (GPa)	G_{12}, G_{31}, G_{23}	7.2 , 7.2 , 7.2
Poisson ratio	$\nu_{12}, \nu_{13}, \nu_{23}$	0.28 , 0.28 , 0.28
Density (kg/m^3)	ρ	1389.23
Coefficients of thermal expansion ($1/^{\circ}C$)	α_1, α_2	11.34 e-6 , 36.9 e-6
Environment temperature ($^{\circ}C$)	T_0	20

Conclusion

In the present work, critical buckling temperatures are obtained using a semi-analytical finite element method. The results have been achieved based on both non-simplified and simplified Sanders theories by calculating geometric stiffness matrix. Based on the numerical results presented in this paper are obtained in the form of tables and figures the following conclusions may be drawn:

1. The results, shows of critical thermal buckling increases with increment of fiber angle.
2. The critical buckling temperature is the highest for fiber angle 75°.
3. Comparison of the results from two different theories shows that the critical thermal buckling temperature based on non-simplified is higher than simplified Sanders theory.
4. The lowest critical buckling temperature is presented for two employed theories which correspond to different mode numbers. One can see no significant changes in mode numbers corresponding to simplified and non simplified sanders theory, expect for the shells with 75 and 90 of fiber angle. This is due to the effect of increment of fiber angles on sanders theories.

Table (3): Validation of the lowest critical buckling temperature for composite cylindrical shell with $l/R = 1.048$.

Fiber angle	lowest critical buckling temperature ($^{\circ}C$)	
	Non Simplified sanders	Simplified Sanders
0	46.96(15) *	45.75(15)
15	62.76(16)	59.33(16)
30	74.76(13)	71.56(13)
60	88.82(9)	88.6(9)
75	159.4(15)	155.2(13)
90	216.2(14)	204.2(8)

* Number in bracket indicate circumferential mode.

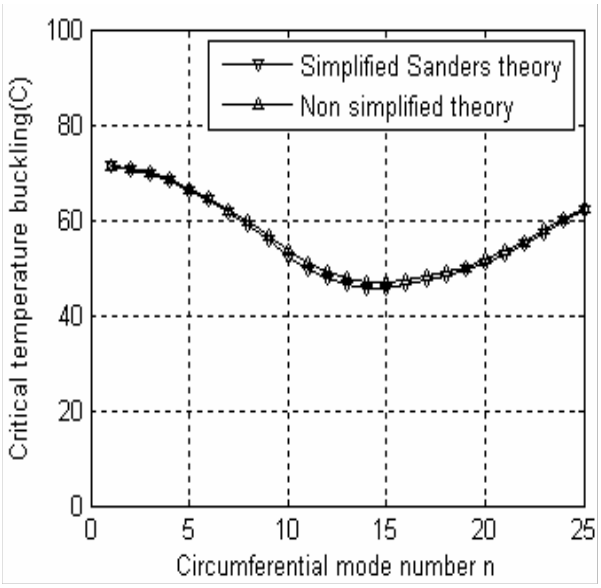

Figure (3): Critical buckling temperatures of the first axial mode associated with 25 harmonic. High strength carbon-Graphite/Epoxy cylindrical shell with fiber angle 0°.

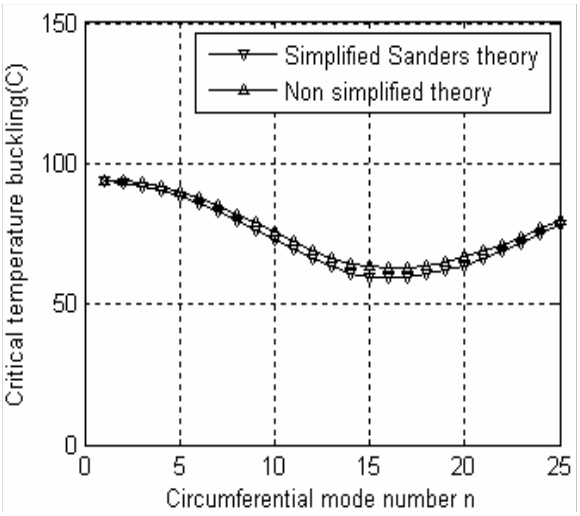

Figure (4): Critical buckling temperatures of the first axial mode associated with 25 harmonic. High strength carbon-Graphite/Epoxy cylindrical shell with fiber angle 15°.

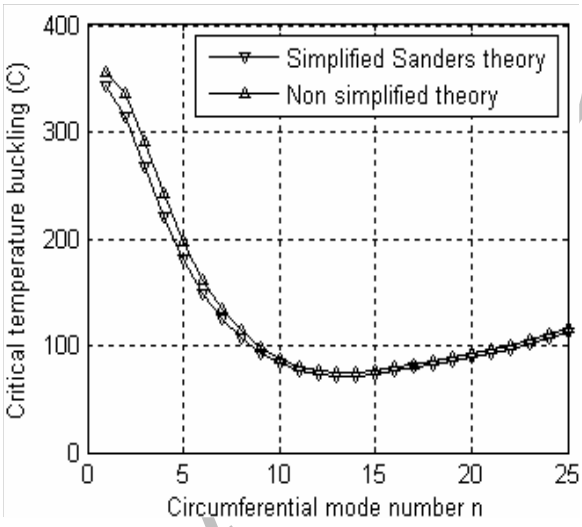

Figure (5): Critical buckling temperatures of the first axial mode associated with 25 harmonic. High strength carbon-Graphite/Epoxy cylindrical shell with fiber angle 30°.

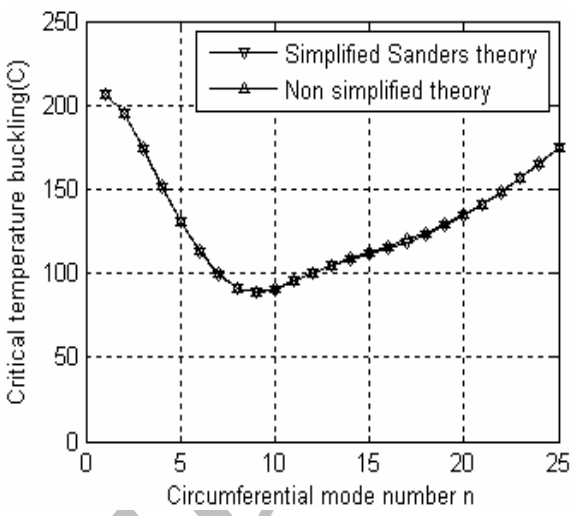

Figure (6): Critical buckling temperatures of the first axial mode associated with 25 harmonic. High strength carbon-Graphite/Epoxy cylindrical shell with fiber angle 60°.

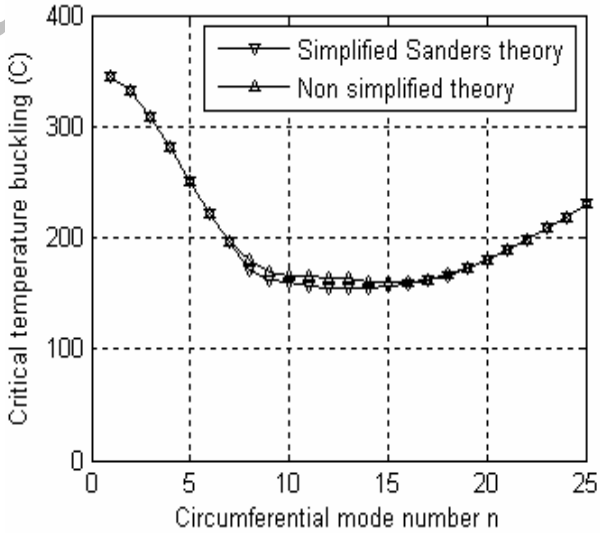

Figure (7): Critical buckling temperatures of the first axial mode associated with 25 harmonic. High strength carbon-Graphite/Epoxy cylindrical shell with fiber angle 75°.

References

1. Thornton, E., "Thermal Buckling of Plates and Shells", Appl Mech Rev., Vol. 46, No. 10, pp.485-506, 1993.
2. Toorani, M.H. and Lakis A.A., "General Equations of Anisotropic Plates and Shells Including Transverse Shear Deformations, Rotary Inertia and Initial Curvatures Effects", J. Sound Vib., Vol. 237, No. 4, pp. 561-615, 2000.
3. Abir, D., and Nadro, A., "Thermal Buckling of Circular Cylindrical Shells Under the Circumferential Temperature Gradients", Aerospace Sci., Vol. 26, No. 6, pp. 803-8, 1959.
4. Patel, B.P., Shukla, K.K., and Nath, Y., "Thermal Buckling of Laminated Cross-Ply Oval Cylindrical Shells", Compos. Struct., Vol. 65, No. 2, pp. 217-29, 2004.
5. Ganesan, N., Kadoli, R., "Buckling and Dynamic Analysis of Piezothermoelastic Composite Cylindrical Shell", J. Compos. Struct., Vol. 59, No. 1, pp. 45-60, 2003.
6. Birman, V., and Bert, C.W., "Buckling and Post-buckling of Composite Plates and Shells Subjected to Elevated Temperature", ASME J. Appl. Mech., Vol. 60, No. 4, pp. 514-9, 1993.
7. Kraus, H., "Thin Elastic Shells", John Wiley & Sons, New York, 1967.

Appendix

$$[B]^T = \begin{bmatrix}
N_1'c & 0 & 0 & 0 & -\frac{n}{R}N_1 s & 0 & 0 & 0 & 0 & 0 \\
0 & N_1's & 0 & \frac{n}{R}N_1 c & 0 & -\frac{1}{R}N_1 s & 0 & 0 & 0 & 0 \\
0 & 0 & N_1'c & \frac{1}{R}N_1 c & 0 & -\frac{n}{R}N_1 s & 0 & 0 & 0 & 0 \\
0 & 0 & N_1 c & 0 & 0 & 0 & N_1'c & 0 & 0 & -\frac{n}{R}N_1 s \\
0 & 0 & 0 & 0 & 0 & N_1 s & 0 & N_1's & \frac{n}{R}N_1 c & 0 \\
N_2'c & 0 & 0 & 0 & -\frac{n}{R}N_2 s & 0 & 0 & 0 & 0 & 0 \\
0 & N_2's & 0 & \frac{n}{R}N_2 c & 0 & -\frac{1}{R}N_2 s & 0 & 0 & 0 & 0 \\
0 & 0 & N_2'c & \frac{1}{R}N_2 c & 0 & -\frac{n}{R}N_2 s & 0 & 0 & 0 & 0 \\
0 & 0 & N_2 c & 0 & 0 & 0 & N_2'c & 0 & 0 & -\frac{n}{R}N_2 s \\
0 & 0 & 0 & 0 & 0 & N_2 s & 0 & N_2's & \frac{n}{R}N_2 c & 0 \\
N_3'c & 0 & 0 & 0 & -\frac{n}{R}N_3 s & 0 & 0 & 0 & 0 & 0 \\
0 & N_3's & 0 & \frac{n}{R}N_3 c & 0 & -\frac{1}{R}N_3 s & 0 & 0 & 0 & 0 \\
0 & 0 & N_3'c & \frac{1}{R}N_3 c & 0 & -\frac{n}{R}N_3 s & 0 & 0 & 0 & 0 \\
0 & 0 & N_3 c & 0 & 0 & 0 & N_3'c & 0 & 0 & -\frac{n}{R}N_3 s \\
0 & 0 & 0 & 0 & 0 & N_3 s & 0 & N_3's & \frac{n}{R}N_3 c & 0
\end{bmatrix}$$

Where, $s = \sin\theta$ and $c = \cos\theta$ and N_1', N_2', N_3' are derivative N_1, N_2, N_3 respect to s.

$$[D] = \begin{bmatrix} G_{11} & G_{16} & 0 & A_{12} & A_{16} & 0 & H_{11} & H_{16} & B_{12} & B_{16} \\ G_{61} & G_{66} & 0 & A_{62} & A_{66} & 0 & H_{61} & H_{66} & B_{62} & B_{66} \\ 0 & 0 & AA_{55} & 0 & 0 & A_{54} & 0 & 0 & 0 & 0 \\ A_{21} & A_{26} & 0 & G'_{22} & G'_{26} & 0 & B_{21} & B_{26} & H'_{22} & H'_{26} \\ A_{61} & A_{66} & 0 & G'_{62} & G'_{66} & 0 & B_{61} & B_{66} & H'_{62} & H'_{66} \\ 0 & 0 & A_{45} & 0 & 0 & BB_{44} & 0 & 0 & 0 & 0 \\ H_{11} & H_{16} & 0 & B_{16} & B_{16} & 0 & J_{11} & J_{16} & D_{12} & D_{16} \\ H_{61} & H_{66} & 0 & B_{66} & B_{66} & 0 & J_{61} & J_{66} & D_{62} & D_{66} \\ B_{21} & B_{26} & 0 & H'_{26} & H'_{26} & 0 & D_{21} & D_{26} & J'_{22} & J'_{26} \\ B_{61} & B_{66} & 0 & H'_{26} & H'_{66} & 0 & D_{61} & D_{66} & J'_{62} & J'_{66} \end{bmatrix},$$

where

$$a_1 = \frac{1}{R_2} - \frac{1}{R_1} \quad , \quad a_2 = \frac{1}{R_1}\left(\frac{1}{R_1} - \frac{1}{R_2}\right) \quad , \quad a_3 = \frac{1}{R_1^2 R_2},$$

$$b_1 = \frac{1}{R_1} - \frac{1}{R_2} \quad , \quad b_2 = \frac{1}{R_2}\left(\frac{1}{R_2} - \frac{1}{R_1}\right) \quad , \quad b_3 = \frac{1}{R_1 R_2^2},$$

and

$$G_{ij} = A_{ij} + a_1 B_{ij} + a_2 D_{ij} + a_3 E_{ij}$$
$$H_{ij} = B_{ij} + a_1 D_{ij} + a_2 E_{ij} + a_3 F_{ij}$$
$$G'_{ij} = A_{ij} + b_1 B_{ij} + b_2 D_{ij} + b_3 E_{ij}$$
$$H'_{ij} = B_{ij} + b_1 D_{ij} + b_2 E_{ij} + b_3 F_{ij}$$
$$J_{ij} = D_{ij} + a_1 E_{ij} + a_2 F_{ij} + a_3 C_{ij}$$
$$J'_{ij} = D_{ij} + b_1 E_{ij} + b_2 F_{ij} + b_3 C_{ij} \qquad i, j = 1,6,2,6$$